Transp Porous Med (2007) 70:231–255
DOI 10.1007/s11242-006-9097-9

ORIGINAL PAPER

Analysis of capillary interaction and oil recovery under ultrasonic waves

Tarek Hamida · Tayfun Babadagli

Received: 14 March 2006 / Accepted: 15 December 2006 / Published online: 10 March 2007

Abstract Although, the effects of ultrasonic irradiation on multiphase flow through porous media have been studied in the past few decades, the physics of the acoustic interaction between fluid and rock is not yet well understood. Various mechanisms may be responsible for enhancing the flow of oil through porous media in the presence of an acoustic field. Capillary related mechanisms are peristaltic transport due to mechanical deformation of the pore walls, reduction of capillary forces due to the destruction of surface films generated across pore boundaries, coalescence of oil drops due to Bjerknes forces, oscillation and excitation of capillary trapped oil drops, forces generated by cavitating bubbles, and sonocapillary effects. Insight into the physical principles governing the mobilization of oil by ultrasonic waves is vital for developing and implementing novel techniques of oil extraction. This paper aims at identifying and analyzing the influence of high-frequency, high-intensity ultrasonic radiation on capillary imbibition. Laboratory experiments were performed using cylindrical Berea sandstone and Indiana limestone samples with all sides (quasi-co-current imbibition), and only one side (counter-current imbibition) contacting with the aqueous phase. The oil saturated cores were placed in an ultrasonic bath, and brought into contact with the aqueous phase. The recovery rate due to capillary imbibition was monitored against time. Air–water, mineral oil–brine, mineral oil–surfactant solution and mineral oil-polymer solution experiments were run each exploring a separate physical process governing acoustic stimulation. Water–air imbibition tests isolate the effect of ultrasound on wettability, capillarity and density, while oil–brine imbibition experiments help outline the ultrasonic effect on viscosity and interfacial interaction between oil, rock and aqueous phase. We find that ultrasonic irradiation enhances

T. Hamida · T. Babadagli(✉)
Department of Civil and Environmental Engineering, School of Mining and Petroleum, University of Alberta, 3-112 Markin CNRL-NREF, Edmonton, AB, Canada T6G 2W2
e-mail: tayfun@ualberta.ca

Present address:
T. Hamida
Alberta Research Council, Edmonton, AB, Canada

capillary imbibition recovery of oil for various fluid pairs, and that such process is dependent on the interfacial tension and density of the fluids. Although more evidence is needed, some runs hint that wettability was not altered substantially under ultrasound. Preliminary analysis of the imbibition recoveries also suggests that ultrasound enhances surfactant solubility and reduce surfactant adsorption onto the rock matrix. Additionally, counter-current experiments involving kerosene and brine in epoxy coated Berea sandstone showed a dramatic decline in recovery. Therefore, the effectiveness of any ultrasonic application may strongly depend on the nature of interaction type, i.e., co- or counter-current flow. A modified form of an exponential model was employed to fit the recovery curves in an attempt to quantify the factors causing the incremental recovery by ultrasonic waves for different fluid pairs and rock types.

Keywords Ultrasonic waves · Oil recovery · Capillary imbibition · Interfacial tension · Capillarity · Surfactants

Nomenclature

A	Cross sectional area
C	Constant
D	Core diameter (cm)
ϕ	Porosity
$f(\gamma,\theta)$	Capillary function
γ	Interfacial tension (dynes/cm)
k	Matrix permeability (millidarcy)
k_w	Permeability to water (millidarcy)
L	Core length (cm)
L_m	Matrix length (cm)
μ_{gm}	Geometric mean of oil and water viscosities (cp)
μ_o	Oil viscosity (cp)
μ_w	Water viscosity(cp)
n	Exponent
$P_{c,\text{eff}}$	Effective capillary pressure (kPa)
PV	Pore volume
Q	Imbibition rate (cm^3/min)
R	Recovery (cm^3)
ρ	Density (g/cm^3)
R_∞	Ultimate recovery (cm^3)
S_w	Water saturation
t	Time (min)
ω	Convergence constant (min^{-n})

Labels

ADA	Alkyldiphenyloxide disulfonic acid
CMC	Critical miscelle concentration
HI	High intensity ($45W/cm^2$)
IFT	Interfacial tension
K	Kerosene

LO	Low intensity (25W/cm^2)
MO	Mineral oil
NUS	No ultrasound
OIIP	Oil initially in place
Surf	Surfactant
US	Ultrasound

1 Introduction

The use of sonic energy to stimulate and enhance oil recovery has been extensively studied in the past four decades. Such stimulation method provides an economically feasible and environmentally friendly alternative to established secondary and tertiary recovery methods. The interest in vibroseismic stimulation dates back to the early 50s when increased oil recovery was observed as a consequence of cultural noise and earthquakes. Beresnev and Johnson (1994) provide an excellent review of the major developments in seismic stimulation in the USA and Russia. Guo et al. (2004) discussed various field tests of seismic application in China. When a seismic (high wavelength) wave passes through fractured porous media, it will disperse into higher harmonics thereby generating waves at ultrasonic frequencies within the reservoir Krylov et al. (1991). Therefore, knowledge of the effect of ultrasound on flow through porous media is relevant to technologies such as pressure pulsing, downhole acoustic stimulation and the use of explosives as form of seismic stimulation.

The potential of ultrasound as a viable method to enhance oil recovery in mature fields was first investigated by Duhon and Campbell (1965). They performed a series of brine flood experiments on oil saturated sandstone samples under ultrasound at a frequency range of 1–5.5 MHz. Their observations showed that ultrasonic energy did have a considerable effect on displacement efficiency by creating a more uniform displacement front. They postulated that ultrasound generates localized pressure surges during cavitation, as well as oscillating air bubbles, which may force trapped oil into adjacent pores.

Later, Fairbanks and Chen (1971) performed a series of experiments testing the effect of heat transfer on the percolation of fluids through porous media under ultrasound. Increase in percolation rate was observed for all cases investigated. Since the temperature strongly affects viscosity, interfacial tension and density of the phases, it was not clear whether the observed improvements were due to temperature or due to the vibrations by ultrasound. Percolation of oil in different porous rock types were also investigated by Mikhailov et al. (1975), Dyblenko et al. (1989), Neretin and Yudin (1981).

Gadiev (1977) introduced ultrasound to oil saturated unconsolidated sand packs and observed considerable increase in oil production rate and cumulative oil production. He postulated that this effect was due to a phenomenon called “sono-capillary effect”, by which the liquid level within a capillary is raised due to an additional pressure generated from collapsing bubbles during cavitation. This effect has been studied by numerous authors (Hilpert et al. 2000; Rozina 2003; Rozina and Rosin 2003; Dezhkunov and Leighton 2004).

Recently, Li et al. (2005) studied the mobilization of oil ganglia in a 2D etched glass micromodel under low frequency vibrations. They observed an increase in the recovery of trichloroethylene (TCE) with higher acceleration amplitude and lower

frequency. They attributed these findings to the fact that vibrations provide the necessary mechanical force to overcome capillary entrapment, thereby mobilizing oil drops within pores. High power ultrasound may also be applied to reduce formation damage caused by fines and drilling mud solids, and to help mobilize clays in rocks (Venkitaraman et al. 1995; Wong et al. 2003, 2004; Roberts et al. 2000; Champion et al. 2004; Poesio et al. 2004), thereby increasing rock permeability and porosity. Venkitaraman et al. (1995) conducted a series of laboratory experiments to investigate the feasibility of using ultrasound to remove formation damage caused by water-based drilling mud and fines. They damaged Berea sandstone and limestone cores with drilling mud, and then treated it with ultrasonic radiation at various frequencies and intensities. After backflow, they found that permeability was greatly increased. Poesio et al. (2004) developed an extensive theoretical model to predict removal of small particles and fines in porous media. Roberts et al. (2000) showed that ultrasonic energy can be effectively applied to reduce near-wellbore damage caused by organic deposits and polymers by suspending paraffin deposits and restoring the effective permeability of the rock. Other applications of ultrasound in porous media are remediation of soil (Iovenitty et al. 1996; Kim and Wang 2003), and mass transfer in textiles (Moholkar and Warmoeskerken 2004). Hamida and Babadagli studied the effect of ultrasound on immiscible (Hamida and Babadagli 2006) and miscible Hamida and Babadagli 2005 displacement on Hele-Shaw cells.

In this study, a series of capillary imbibition experiments under ultrasound were conducted on sandstone plugs using a focused ultrasonic beam. The aim was twofold: (a) to identify the governing mechanisms and correlate their relative effects on ultimate recovery and production rate of oil, and (b) to investigate the capillary interaction phenomenon under ultrasonic waves.

2 Oil recovery mechanisms under sonic waves

Despite extensive research on ultrasonic stimulation of flow through porous media, and various field trials and patents (Pechkov et al. U.S. patent; Ellingsen et al. U.S. patent; Wegener et al. U.S. patent; Meyer et al. U.S. patent), the exact mechanism is yet not well understood. Ultrasonic radiation introduces mechanical vibrations, which strongly influence interfacial and viscous forces by enhancing momentum and heat transfer across the phase interfaces. The following mechanisms are believed to be responsible for the observed improvement in percolation of oil within porous media:

- Increase in relative permeability of the phases (Cherskiy et al. 1977; Nikolaevskiy, 1989).
- Nonlinear acoustic effects such as in-pore turbulence, acoustic streaming, cavitation, and perturbation in local pressures. Such effects reduce the adherence of wetting films onto the rock matrix and may only be relevant at high ultrasonic intensities.
- Reduction of surface tension, density and viscosity as a consequence of heating by ultrasonic radiation. Ultrasound may also be very effective in reducing viscosity of thixotropic fluids,
- Mechanical vibration of pore walls initiate peristaltic transport, by which fluid is "squeezed" into adjacent pores (Aarts and Ooms 1998; Aarts et al. 1999),

- Micro-emulsification of oil in the presence of natural or introduced surfactants (Abismail et al. 1999),
- Coalescence and dispersion of oil drops due to the Bjerknes forces (Bjerknes 1906; Metting et al. 1997),
- Increase in rock permeability and porosity due to removal of fines and clays, paraffin wax and asphaltenes (Roberts et al. 2000; Champion et al. 2004; Wong et al. 2004; Poesio et al. 2004),
- Oscillation and excitation of capillary trapped oil drops due to pressure perturbations generated by cavitating bubbles and mechanical vibrations of rock and fluid (Graham and Higdon 2000a, b, 2002a, b).

These mechanisms, which are predominantly controlled by capillary and viscous forces, depend on the frequency and intensity of the ultrasound, as well as rock elasticity, fluid properties, porosity, cementation, and clay content. At higher intensity, mechanical stresses, and therefore, temperature increase. Frequency plays an important role in wave dispersion, attenuation and heat dissipation. An analytical treatment of compressional and shear wave propagation in saturated porous media was first developed in the two classic papers by Biot (1956a, b). Extensions of the theory of compressional waves in porous media were developed by numerous researchers, most notably Buckingham (1999) and Aarts and Ooms (1998).

3 Experimental study

3.1 Rock and fluid properties

Cylindrical plugs taken from a block of homogeneous Berea sandstone and Indiana limestone were used in experiments. Properties and dimensions of all cores are provided in Table 1. Some of the samples were coated with epoxy from all sides except one of the ends to obtain truly counter-current imbibition. Pore volume was estimated by weighing the mass change before and after saturation and dividing it by density. The fraction of pore volume over bulk core volume yields the fluid porosity. All cores have been used only once to avoid undesirable alterations in wettablitity and grain structure due to contamination, cleaning, and matrix damage generated by ultrasonic vibrations.

Three types of non-wetting fluids were employed; mineral oil, kerosene, and air. To isolate the effect of ultrasound on viscosity, density, interfacial tension, wettability and viscosity, solutions of water, brine (15,000 ppm NaCl), anionic surfactant (alkyldiphenyloxide disulfonic acid), non-ionic surfactant (Alcohol Ethoxylate) or polymer (Xanthan Gum) were prepared as the aqueous phase, respectively. The properties of the fluids at standard conditions (no ultrasound) are presented in Table 2. To avoid ultrasonic cavitation at the core wall, all solutions were carefully de-aerated (with a few exceptions).

Reduction of interfacial tension was achieved by adding different volumes of surfactant to de-aerated water. The CMC of such mixture was measured to occur at a concentration of about 3%. Viscosity of the aqueous phase was increased by adding 0.03 wt.% and 0.09 wt.% of polymer (Xanthan gum) to de-aerated, distilled water. Brine solutions were obtained by mixing 15,000 ppm of NaCl with de-aerated water. We applied an oil base coloring agent to both kerosene and mineral oil to distinguish the fluids from the water.

Table 1 Core properties and dimensions

Core #	Rock type	Coating	PV (cm^3)	ϕ	k (mD)	D (cm)	L (cm)
B1	B	C	5.26	21.01%	200	2.5	5.1
B2	B	C	5.26	21.01%	200	2.5	5.1
L1	L	C	4.26	17.02%	7	2.5	5.1
L2	L	C	4.26	17.02%	7	2.5	5.1
7A	B	UC	5.23	20.89%	200	2.5	5.1
7B	B	UC	5.1	20.78%	200	2.5	5
8A	B	UC	5.43	20.87%	200	2.5	5.3
8B	B	UC	5.3	21.17%	200	2.5	5.1
3A	B	UC	5.43	20.87%	200	2.5	5.3
3B	B	UC	5.51	21.18%	200	2.5	5.3
4A	B	UC	5.34	20.92%	200	2.5	5.2
4B	B	UC	5.23	20.89%	200	2.5	5.1
5A	B	UC	5.38	21.08%	200	2.5	5.2
5B	B	UC	5.5	21.14%	200	2.5	5.3
9A	B	UC	5	20.79%	200	2.5	4.9
9B	B	UC	4.96	21.05%	200	2.5	4.8
6A	B	UC	5.5	21.14%	200	2.5	5.3
6B	B	UC	5.42	20.83%	200	2.5	5.3
10A	B	UC	4.84	20.98%	200	2.5	4.7
10B	B	UC	4.98	21.14%	200	2.5	4.8
B1b	B	C	5.26	21.01%	200	2.5	5.1
B2b	B	C	5.26	21.01%	200	2.5	5.1
B3	B	C	5.26	21.01%	200	2.5	5.1
B4	B	C	5.26	21.01%	200	2.5	5.1
1_1	B	UC	14.9	22.53%	200	3.81	5.8
1_2	B	UC	12.57	21.62%	200	3.81	5.1
2_1	B	UC	12.97	21.88%	200	3.81	5.2
2_2	B	UC	12.7	21.42%	200	3.81	5.2
M1	B	UC	5.96	22.08%	500	2.5	5.5
M2	B	UC	6.22	21.85%	500	2.5	5.8
MM1	B	UC	6.92	23.89%	500	2.5	5.9
MM2	B	UC	6.19	23.35%	500	2.5	5.4
P1	B	UC	5.98	23.89%	500	2.5	5.1
P2	B	UC	6.29	24.64%	500	2.5	5.2
G1	B	UC	6.32	23.41%	500	2.5	5.5
G2	B	UC	6.27	22.81%	500	2.5	5.6
K2	B	UC	6.03	23.18%	500	2.5	5.3
LL2	B	UC	6.11	22.63%	500	2.5	5.5
F1	B	UC	5.94	22.00%	500	2.5	5.5
F2	B	UC	6.5	23.65%	500	2.5	5.6
H1	B	UC	6.26	21.99%	500	2.5	5.8
H2	B	UC	6.24	23.54%	500	2.5	5.4
D1	B	UC	6.24	23.54%	500	2.5	5.4
D2	B	UC	6.28	24.14%	500	2.5	5.3
E1	B	UC	6.26	22.77%	500	2.5	5.6
E2	B	UC	5.52	22.05%	500	2.5	5.1

B: Berea sandstone, L: Indiana limestone, C: coated, UC: uncoated, PV: pore volume

Table 2 Fluid properties of oleic and aqueous phases used in the imbibition experiments

Fluid type	Property	
Light mineral oil (MO):	$\mu = 35.5$ cp	
	$\rho = 0.8125$ g/cc	
	$\sigma_{MO-water} = 32$ dynes/cm	
Kerosene (K):	$\mu = 2.9$ cp	
	$\rho = 0.75$ g/cc	
	$\sigma_{K-water} = 49$ dynes/cm	
Water	$\mu = 1.0$ cp	
	ρ=1.0 g/cc	
	σ = 72.6 dynes/cm	
Anionic surfactant	$\mu = 2.5$ cp	
(alkyldiphenyloxide disulfonic acid)	ρ=1.005 g/cc	
	CMC @ 25°C = (3% vol.)	
	$\sigma_{MO} = 10$ dynes/cm (3% vol.)	
Nonionic surfactant	$\mu = 1.5$ cp	
(ethoxylated alcohol)	$\rho = 0.99$ g/cc	
	CMC @ 25°C = 39 ppm	
	pH (1 vol.%) = 6.8	
	$\sigma_{MO-surf} = 10$ dynes/cm (1 vol. %)	
	$\sigma_{K-surf} = 3$ dynes/cm (1 vol. %)	
Fluid pairs	Interfacial tension[1] (dynes/cm)	
Water + 15,000 ppm NaCl	70.5 ± 1.4	
Water + 1% DOWFAX 2A1	33.8 ± 0.7	
Water + 3% DOWFAX 2A1	34.1 ± 0.7	
Water + 5% DOWFAX 2A1	34.6 + 0.7	
Water + 0.1% TERGITOL 15-S-7	30.1 ± 0.6	
Water + 0.5% TERGITOL 15-S-7	27.8 + 0.6	
Water + 1.0% TERGITOL 15-S-7	27.5 ± 0.6	
Water + 0.03% Xanthan gum	68.0 + 3.4	
Water + 0.05% Xanthan gum	66.5 + 3.3	
Water + 0.1% Xanthan gum	65.0 ± 3.3	
Light mineral oil	31.5 ± 0.6	
Kerosene	27.2 + 0.5	
Heavy fluid	Light fluid	Interfacial tension (dynes/cm)
Water	Air	71.0 ± 1.4
1% DOWFAX 2A1	Air	33.8 ± 0.7
3% DOWFAX 2A1	Air	34.1 ± 0.7
5% DOWFAX 2A1	Air	34.6 ± 0.7
0.1% TERGITOL 15-S-7	Air	30.1 ± 0.6
0.5% TERGITOL 15-S-7	Air	27.8 ± 0.6
1.0% TERGITOL 15-S-7	Air	27.5 ± 0.6
15,000 ppm NaCl	Air	70.5 ± 1.4
Water	Light MO	61.8 ± 1.2
15,000 ppm NaCl	Light MO	53.2 ± 1.1
1% DOWFAX 2A1	Light MO	10.1 ± 0.2
3% DOWFAX 2A1	Light MO	11.2 ± 0.2
5% DOWFAX 2A1	Light MO	12.0 ± 0.2
0.1% TERGITOL 15-S-7	Light MO	8.6 ± 0.2
0.5% TERGITOL 15-S-7	Light MO	8.2 ± 0.2
1.0% TERGITOL 15-S-7	Light MO	8.1 ± 0.2
0.05% Xanthan gum	Light MO	56.0 ± 1.1
0.1% Xanthan gum	Light MO	53.3 ± 1.1
Water	Kerosene	40.7 ± 0.8
5% DOWFAX 2A1	Kerosene	10.4 ± 0.2
1.0% TERGITOL	Kerosene	6.9 ± 0.1

[1] Measured using a Du Nouy type tensiometer (Fisher Scientific Tensiometer; Platinum-Iridium ring)

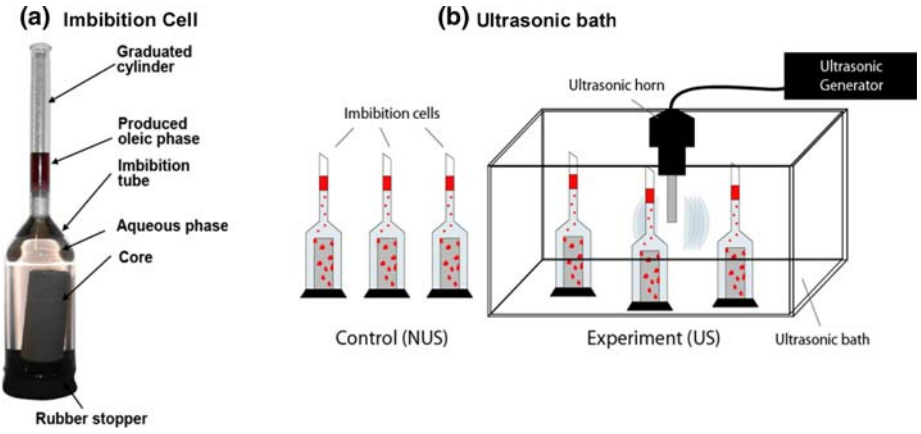

Fig. 1 The main components of the imbibition experiment: (**a**) The imbibition cell, (**b**) the ultrasonic bath and ultrasonic horn

The interfacial tension between aqueous phase and non-wetting phase was measured using a standard tungsten ring tensiometer (the Du Nouy method). Error in interfacial tension was found to be ±7%. The viscosity values were either measured or obtained from the manufacturer. Error in viscosity data is estimated to be less than ±1%. Density values were measured by weighing a known volume of the fluid (5 cm^3), and are accurate to ±0.05 g/cm^3.

3.2 Equipment

The experimental setup is shown in Fig. 1. Cores were placed inside glass imbibition tubes with a graduated cylinder allowing volume measurements with a precision of ±0.1 cm^3. A homogeneous ultrasonic field was generated using a benchtop ultrasonic bath (Branson cleaner) operating at 40 kHz. To investigate the effect of beam sonication, an ultrasonic horn that is capable of generating a frequency of 20 kHz and focused power up to 250 W/cm^2 was used in some experiments (Misonix S3000 Sonicator). The horn was equipped with a 3/4 in. titanium alloy tip, and calibrated calorimetrically. Imbibition cells were positioned equidistantly from the horn. All aqueous phases were carefully de-aerated to avoid cavitation. Since the samples were positioned at equal distance, and used the same imbibition cells, attenuation due to carrying fluid and imbibition cells is negligible. Each experiment was repeated without ultrasound (control experiment using cores from the same block). The relative performance was then compared and analyzed.

The temperature within the ultrasonic bath increases with exposure time due to the high power output of the horn. This increase may influence the experimental results slightly by reducing the viscosity and interfacial tension of the fluids. A plot of chamber temperature versus time for 25 W/cm^2 (LO) and 45 W/cm^2 (HI) is shown in Fig. 2. We observed that the temperature increases logarithmically with time. In a period of 750 min, the temperature within the ultrasonic bath rose from 20°C to 24°C at 25 W/cm^2, and from 21°C to 29.5°C at 45 W/cm^2. Considering the thermal

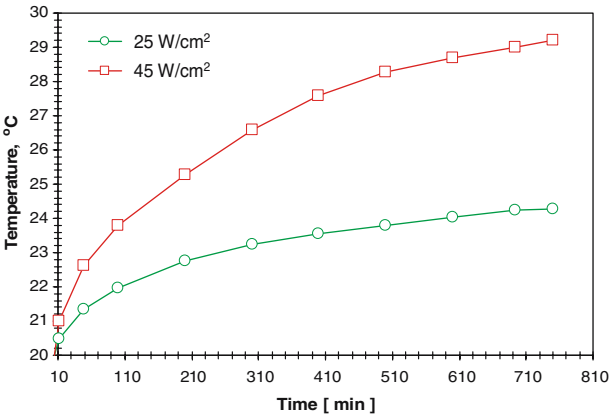

Fig. 2 Temperature change within the ultrasonic container at 25 W/cm^2 (LO) and 45 W/cm^2 (HI) power output

Table 3 Thermal properties of oleic and aqueous phases within the range of ultrasonic heating

	CAS#	Isothermal heat surface tension viscosity expansion			
		10^3	/°C	mN/m	mPa s
Water	7732-18.	20	0.206	72.702	0.963
		25	0.256	71.99	0.89
		30	0.302	71.125	0.771
Kerosene	8008-20.	20	0.99	27.2	2.5
		25	0.99	25	2.1–2.2
Light mineral oil	8042-47	20	0.98	31.5–35.5	46.5
		30	0.99	–	40

properties of the fluids ulated in Table 3, the expansion of the pores and alterations of fluid properties due to this temperature change was considered negligible.

3.3 Procedure

Dry cores were positioned in a vacuum desiccator filled with the oleic phase, and allowed to saturate for 2 days. The saturated cores were then weighed and placed inside the imbibition cell. A rubber stopper was used to seal off the bottom of the imbibition cell. After ensuring that the imbibition cell was leak tight, the aqueous phase was slowly introduced via a funnel. The recovery due to spontaneous imbibition was recorded versus time with and without ultrasound. Ultrasound was applied at two intensities: 25 and 45 W/cm^2. Occasionally, the cores were weighed using a string attached to a hook on a portable scale to verify that the volumes measured from the graduated imbibition tube match the change in mass due to fluid influx. The resulting recovery curves are presented in Fig. 3. In some of the surfactant experiments, we observed a stable emulsion, which increased the measured volume of produced fluid. In such case, volumes were corrected from the weight of the cores. Error in recorded volume is approximately ±5%. For every reading, the cores were carefully shaken to liberate any oil drops that remained attached to the core wall. On average,

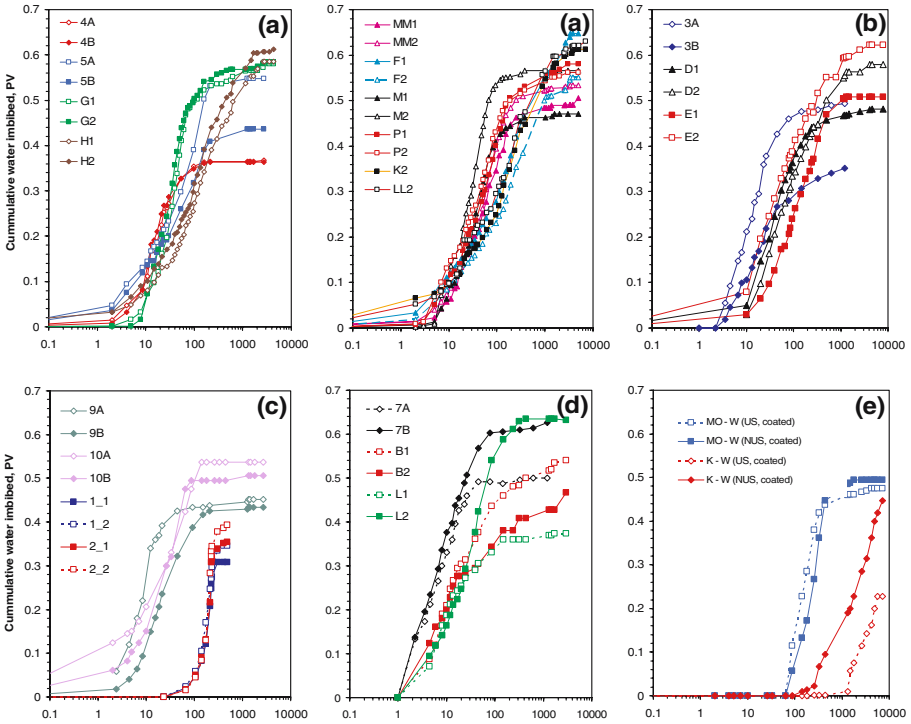

Fig. 3 Raw data-recovery curves for all imbibition experiments: (**a**) mineral oil–surfactant, (**b**) mineral oil–brine, (c) kerosene–brine, kerosene–surfactant, mineral oil–polymer, (**d**) air–water in coated sandstone and uncoated limestone and (**e**) kerosene–brine and mineral oilbrine in coated sandstone (see Table 4 for experiment types). Hollow symbols represent ultrasonically enhanced imbibition (US) and filled symbols indicate the cases without ultrasonic energy (NUS)

the volumes obtained by weighing the cores agree with the volumetric recording to approximately 7% accuracy. The list of experiments is given in Table 4.

4 Analysis of results

4.1 Qualitative analysis

A plot of final recovery without ultrasound versus final recovery with ultrasound is shown in Fig. 4, which was generated using the oil recovery curves given in Fig. 3. The solid line represents the case when ultrasound and no ultrasound perform equally. Dashed lines indicate the regions of 10%, 20%, and 30% deviation from the control. Almost all experiments demonstrated an enhancement of final recovery under ultrasonic waves. Exceptions include some counter-current experiments, air–water (7A, 7B), and mineral oil–surfactant at 14% concentration (H1, H2). For those experiments, we observed a lower ultimate recovery under ultrasound. In case of 14% ADA, the reduced production may be due to the intrinsically different rheological properties

Table 4 Experimental matrix of imbibition experiments

Phase		Core#	Coating
nw	w		
A	DAW	B1, B2	C
A	DAW	L1, L2	C
A	DAW	7A, 7B	UC
A	AW	8A, 8B	UC
MO	B	3A, 3B	UC
MO	S (1%)	4A, 4B	UC
MO	S (5%)	5A, 5B	UC
K	DAW	9A, 9B	UC
K	S (5%)	10A, 10B	UC
MO	DAW	B1b, B2b	C
K	DAW	B3, B4	C
MO	P (0.03%)	1-1, 1-2	UC
MO	P (0.09%)	2-1, 2-2	UC
MO	S (1%)	M1, M2	UC
MO	S (2%)	MM1, MM2	UC
MO	S (3%)	P1, P2	UC
MO	S (4.8%)	G1, G2	UC
MO	S (9%)	K2, LL2	UC
MO	S (9%)	F1, F2	UC
MO	S (14.3%)	H1, H2	UC
MO	B	D1, D2	UC
MO	B	E1, E2	UC

B: Berea sandstone, L: Indiana limestone, DAW: De-aerated water, AW: aerated water, A: air, K: kerosene, MO: mineral oil, P: polymer, B: brine, S: surfactant, C: coated, UC: uncoated, nw: non-wetting, w: wetting

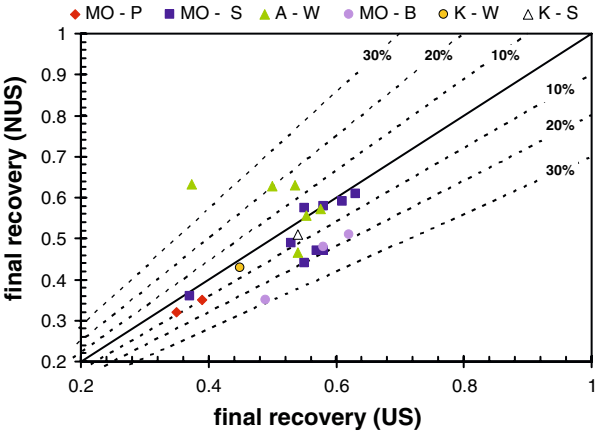

Fig. 4 Plot of final recovery of undisturbed imbibition (NUS) versus imbibition by ultrasound (US) for various fluid pairs. The solid line indicates the "no difference" scenario. Dashed lines represent percentual deviation from "no difference". The definitions for the abbreviations are provided in Table 4

of oil in water microemulsions that form at such high surfactant concentrations and ultrasonic vibrations.

Counter-current and co-current air–water imbibition into Berea sandstone (Fig. 5) was significantly enhanced under ultrasound, yielding an additional recovery of up to 10% PV. The rate of imbibition remained unchanged for the co-current boundary conditions, but was substantially improved for the counter-current case. A similar, but less substantial change in recovery was observed with air–water imbibition into

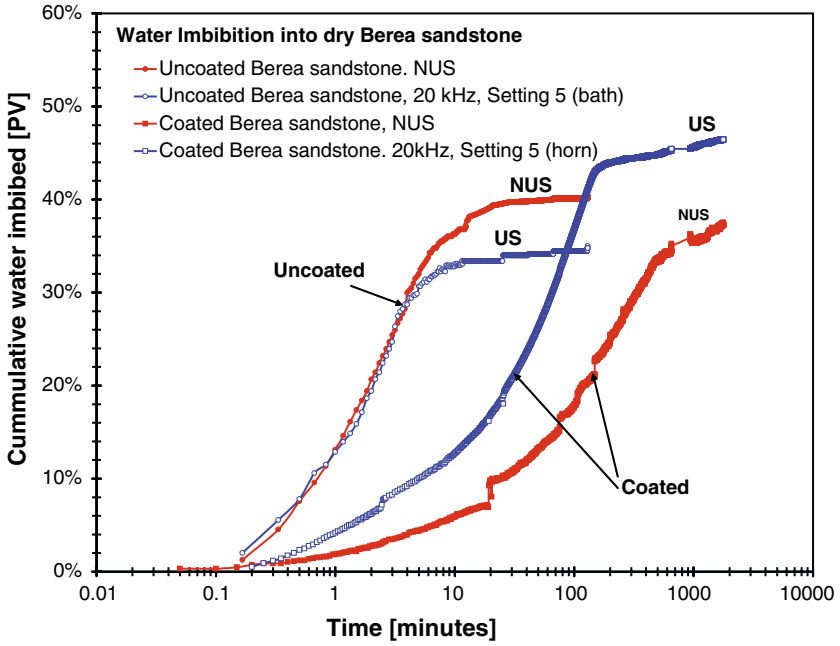

Fig. 5 Air–water imbibition in Berea sandstone under ultrasonic irradiation with an ultrasonic horn (20 kHz, 48 W/cm^2) and an ultrasonic bath (40 kHz, 2kW). Adapted from Hamida and Babadagli (2005)

limestone (Fig. 6). Ultrasonic treatment via a horn (45 W/cm^2) reduced the recovery in uncoated limestone by approximately 9%, but increased the recovery in coated limestone by 11%. One reason for these observed changes in recovery and recovery rate may be due to resonating air bubbles which are trapped in the pores. Bubbles strongly affect the acoustic properties of liquids due to the large contrast in compressibility and viscosity of the gas and liquid. Predominant features in a liquid with suspended bubbles are high dispersion and low sound speeds over a wide range of frequencies. Bubbles trapped in porous media may oscillate with ultrasound, and absorb most of the ultrasonic energy (Herskowitz et al. 2000). Since the transport of aqueous phase in water-wet Berea is along the pore-walls, the vibrating bubbles do not greatly interfere with the co-current nature of the flow. On the other hand, for counter-current flow within Berea sandstone, the vibrational energy of the bubbles may improve flow of air (slip effect), and accelerate the percolation process. Additionally, as observed by Aarts and Ooms (1999), compressibility of the liquid within porous media has a strong influence on the net induced flow caused by transversal wave deformations of the pore-walls. In the case of limestone, which is less water wet, water in the pores competes with the resonating bubbles, and therefore results in less effective imbibition.

Figure 7 shows the recovery curves for mineral oil–brine imbibition at 25 and 45 W/cm^2 using the ultrasonic horn. The control experiment (NUS) recovered 35% OIIP at a rate of 0.06% per minute. Ultrasound at 25 W/cm^2 did not dramatically alter the recovery rate, but increased the ultimate recovery by an additional 5% OIIP. Higher intensity ultrasound caused a greater increase in final recovery up to an

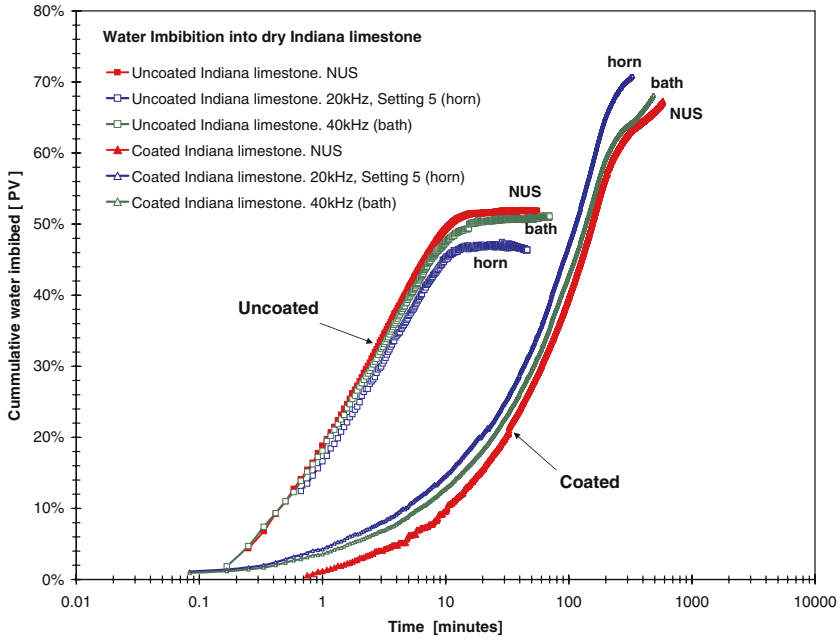

Fig. 6 Air–water imbibition in Indiana limestone under ultrasonic irradiation with an ultrasonic horn (20 kHz, 48 W/cm^2) and an ultrasonic bath (40kHz, 2kW). Adapted from Hamida and Babadagli (2005)

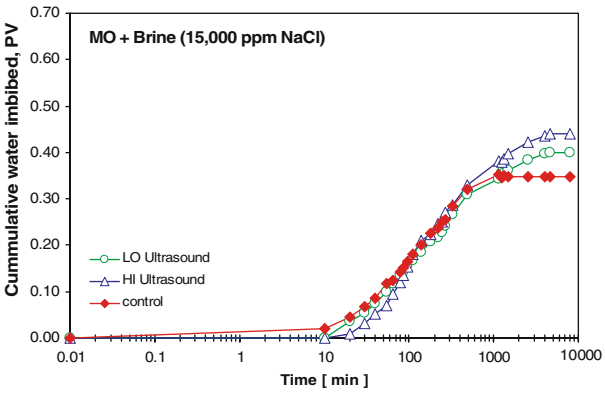

Fig. 7 Recovery curves of mineral oil–brine (15,000 ppm NaCl) using an ultrasonic horn at two intensities; LO = 25 W/cm^2 and HI = 45 W/cm^2

additional 9% OIIP. One possible mechanism responsible for this additional recovery is a more stable displacement front due to pore vibrations and localized pressure perturbations. When the cores were swapped, so that the un-sonicated control cores are subjected to ultrasound and the ultrasonically stimulated cores were removed from the ultrasonic field, no considerable increase in recovery was observed. Therefore, ultrasound did not improve the mobilility of unswept oil once the imbibition process has ceased.

Figure 8(a, b) provide recovery curves of mineral oil with different alkyldiphenyloxide disulfonic acid (ADA) concentrations in Berea sandstone. At both 1% (Fig. 8a)

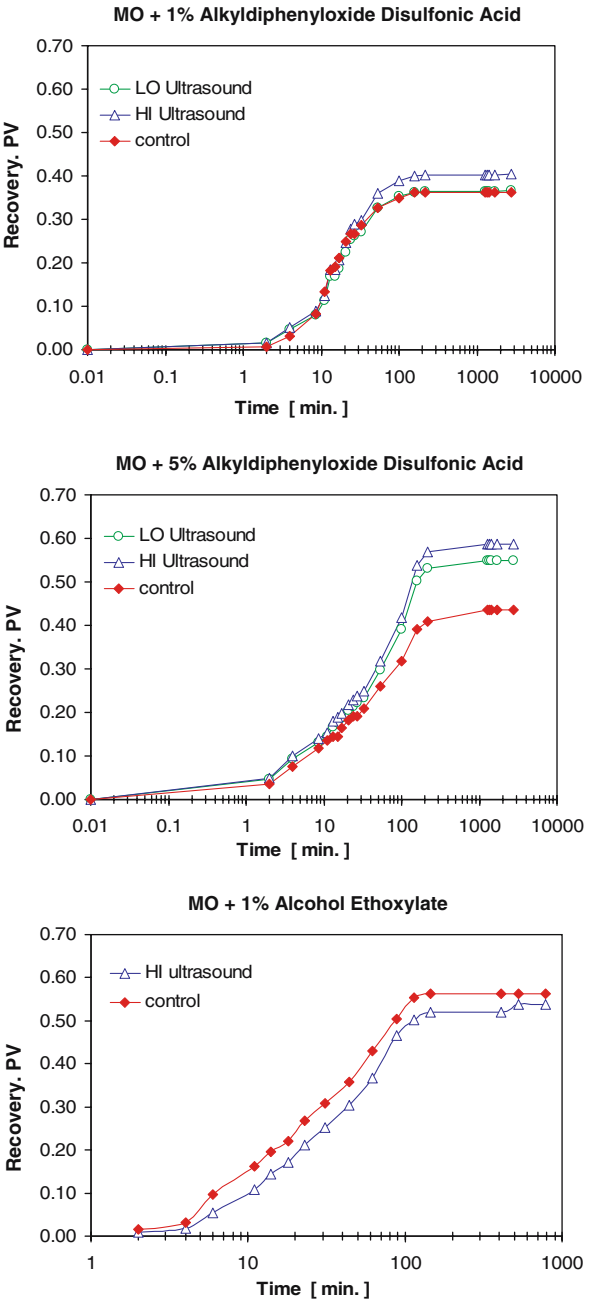

Fig. 8 Recovery curves of (**a**) mineral oil–1% alkyldiphenyloxide disulfonic acid, (**b**) mineral oil–5% alkyldiphenyloxide disulfonic acid and (**c**) mineral oil–1% nonionic ethoxylated alcohol pair at two ultrasonic intensities; LO = 25 W/cm^2 and HI = 45 W/cm^2

and 5% (Fig. 8b) ADA concentrations, the recovery of mineral oil increased by 8% as ultrasonic intensity was almost doubled. For 1% surfactant, the incremental oil produced due to ultrasound and production rate was not substantial. On the other hand, 5% surfactant (above CMC) imbibition under ultrasound showed a substantial increase in ultimate recovery (up to 11% incremental oil) and production rate, when compared to no ultrasound scenario (NUS). Possible explanations for this phenomenon are:

1. Ultrasound may increase solubility of surfactant into the oil, thereby strongly decreasing the interfacial tension. A decrease in interfacial tension will reduce the capillary pressure generated by trapped oil droplets in pores, and thus mobilize oil more effectively.
2. Surfactant adsorption onto the rock matrix: Ultrasound may reduce the surfactant adsorption rate onto the sandstone matrix as a consequence of increasing the solubility of the surfactant, resulting in weakening of the surface films generated at the pore throats. This process may be more severe with anionic surfactants than with nonionic surfactants.
3. Development of micro-emulsion (micelles) under ultrasound. Just after 100 min, we observed that the surfactant solution changed into a semi transparent, foggy micro-emulsion. Therefore, operating ultrasound at surfactant concentrations above CMC accelerates the generation of micelles which may enhance oil recovery.

To test for the conjecture that ultrasound reduces adsorption to the rock matrix by enhancing surfactant solubility, we ran imbibition tests with a 1% Nonionic Ethoxylated Alcohol (post-CMC) solution on mineral oil and kerosene saturated cores. The adsorption levels for both anionic and nonionic surfactants are similar in magnitude, however, adsorption of nonionic surfactants on sandstone is usually higher, and is relatively insensitive to solution salinity. The opposite is true for anionic surfactants, for which negligible adsorption was observed in sulfonates containing alkyl chains shorter than 9 (Trogus and Sophany 1977; Lawson 1978). Mannhardt and Jha (1994) studied the adsorption of anionic surfactants in Berea sandstone at various temperatures and salinity, and found that adsorption increases with decreasing surfactant solubility. Varadaraj et al. (1994) investigated the wettability alteration caused by various surfactant types, and found that wetting rate is higher for ethoxylates than for sulfates, while wetting effectiveness was higher for sulfates. Figure 8(c) shows the resulting recovery curves of 1% Ethoxylated Alcohol imbibition into Berea sandstone saturated with light mineral oil. Although, 5 vol.% ADA and 1 vol.% Ethoxylated Alcohol concentrations are both significantly higher than the CMC, the latter demonstrated very little alteration of both recovery rate and ultimate recovery when ultrasound is applied. Since interfacial tension of both solutions is relatively similar, it cannot be the dominating factor in this imbibition process. Micro-emulsions were produced in both cases, as well. Therefore, micelles cannot be contributing to the significant difference either. The governing mechanism must be controlled by a sensitive interplay between the increase in surfactant solubility and decrease in adsorption due to ultrasonic mixing.

Recovery of kerosene using 5% ADA yielded contrasting results, depending on the ultrasonic intensity applied (Fig. 9). At 25 W/cm^2, both the recovery rate and ultimate recovery were improved as compared to the control. Recovery rate at 45 W/cm^2 did not deviate greatly from that measured at 20 W/cm^2. However, initiation time and ultimate recovery were considerably lower. When ultrasound was removed, additional 14% incremental oil was recovered and ultimate recovery was comparable to

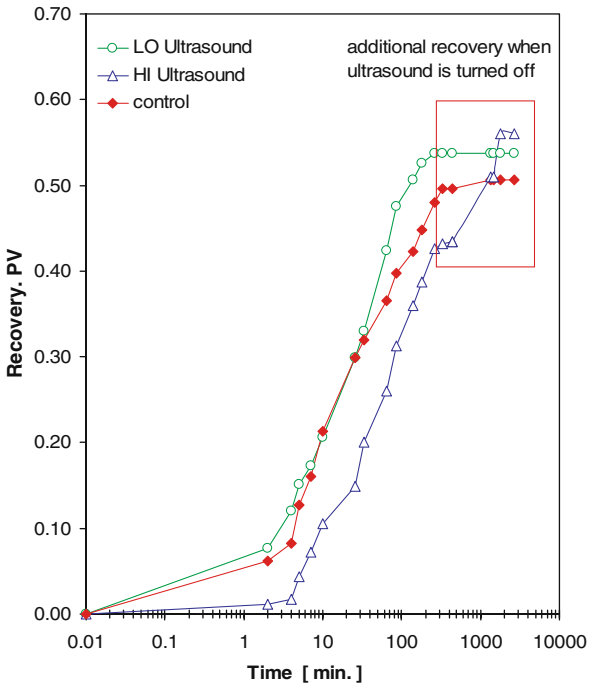

Fig. 9 Recovery curves of kerosene–5%alkyldiphenyloxide disulfonic acid pair at two ultrasonic intensities; LO = 25 W/cm^2 and HI = 45 W/cm^2. The box highlights the incremental recovery of kerosene when ultrasound is discontinued

the value obtained at lower intensity. This behavior was also observed in the counter-current case (sample coated with epoxy from the all sides except the bottom surface) (Fig. 10). Kerosene exhibited a slower production rate compared to mineral oil in both ultrasound and NUS. Ultimate recovery of the sonicated cores is found to be approximately 30% OIIP. When ultrasound is discontinued, we noted a dramatic increase in kerosene production (additional 14% OIIP) but no discernable improvement with mineral oil. When the mineral oil–water control sample was introduced to the ultrasonic field, we observed an additional 4% incremental recovery (tertiary recovery), while the production from the kerosene control remained unchanged. Due to the nature of entirely counter-current flow, it is very likely that the significantly lower interfacial tension of kerosene compared to mineral oil is responsible of the observed phenomenon. Low interfacial tension kerosene ganglia that are trapped in pores may generate additional pressure fields while oscillating (due to their stability), preventing brine from imbibing effectively into the rock matrix.

Figure 11(a, b) show recovery curves of mineral oil imbibing into Berea sandstone at two concentrations of Xanthan gum. At a concentration of 0.03%, ultrasonic irradiation improved the recovery of oil by more than 12%. We observed a direct proportionality between the ultrasonic intensity and final recovery. This is not the case for Xanthan gum at 0.09% concentration. Here, the low intensity ultrasound proved to be more effective at recovering oil by imbibition. This result may be explained by considering the polymer structure of Xanthan gum. Xanthan gum is an anionic polysaccharide string with a cellulose backbone and trisaccharide side chains and repeating pentasaccharide units. When contacting with water, Xanthan gum forms alpha helicies as a secondary structure, which entangele and bind the water molecules. High frequency vibrations by ultrasound increase the entanglement, and cause the helixes

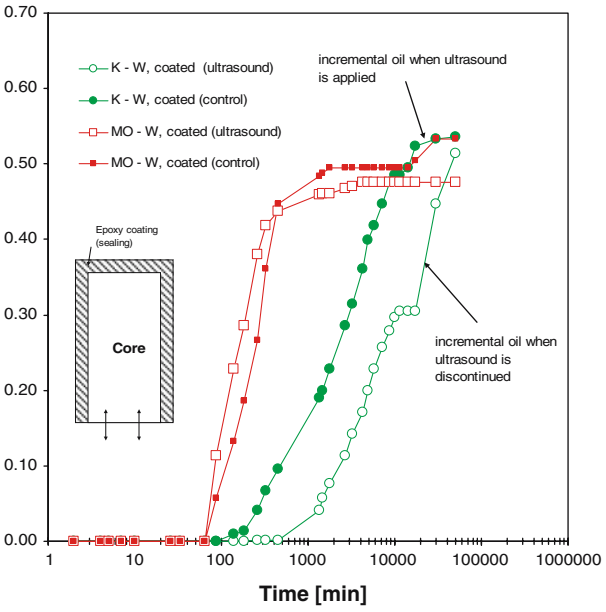

Fig. 10 Recovery curves of counter-current imbibition in coated Berea sandstone with mineral oil and kerosene as oleic phase and 1% alkyldiphenyloxide disulfonic acid as aqueous phase. The ultrasonic intensity is 25 W/cm^2. The embedded drawing shows the geometry of the core plug with 3 of 4 sides coated with epoxy to force counter-current flow. The circled area shows oil production when imbibition cells are reversed

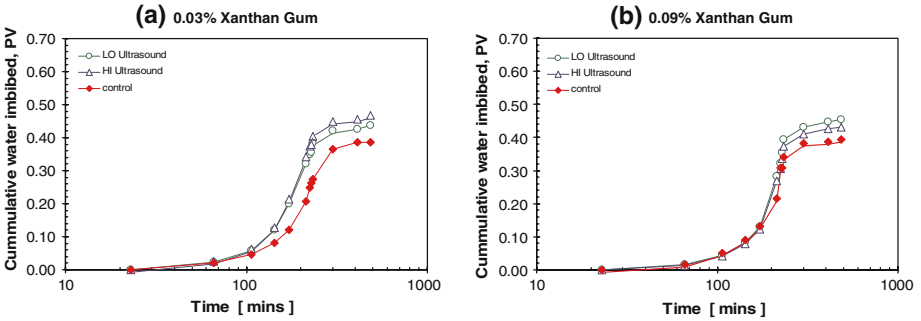

Fig. 11 (**a**) Recovery curves of (**a**) mineral oil–0.03% Xanthan gum and (**b**) mineral oil–0.09% Xanthan gum at two ultrasonic intensities; LO = 25 W/cm^2 and HI = 45 W/cm^2

to vibrate. These vibrations may reduce the mobility of the fluid within the pores. On the other hand, ultrasound homogenizes the mixture and prevents the formation of suspensions and flocculation. An optimum concentration between 0.03% and 0.09% for which ultrasound at high intensity is the most effective is expected. This part of the research is on-going.

Figure 12 summarizes ultimate recoveries at various ultrasonic intensities for each fluid pair. In all cases, except for the 0.09% Xanthan gum solution, ultrasound enhances recovery of oil in direct proportionality to the intensity applied.

4.2 Quantitative analysis

To analyze the effect of ultrasound on co-current and counter-current imbibition in Berea sandstone and Indiana limestone, we utilized a generalized form of the exponential transfer function proposed by Cil et al. (1998):

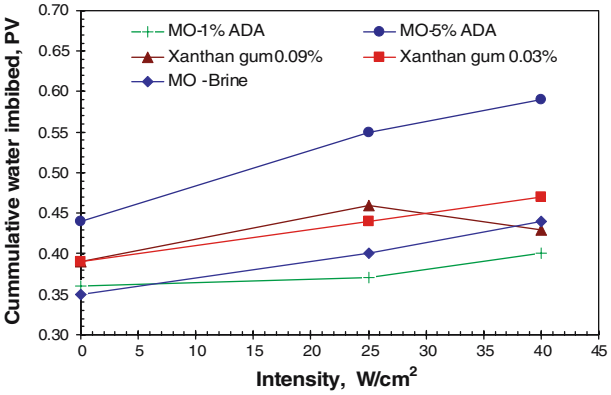

Fig. 12 Ultimate recovery versus ultrasonic energy for various fluid pairs

$$\frac{R}{R_\infty} = 1 - e^{-\omega t^n} \tag{1}$$

where ω and n are parameters controlling the capillary imbibition rate and depend on the rock and fluid properties. This function was observed to give a good match to capillary imbibition recovery data previously (Babadagli et al. 2005). For detailed discussion on the use of this equation to derive a matrix-fracture transfer function, readers are referred to this particular reference. Equation 1 was matched to the curves shown in Fig. 3. The values of ω and n that gives the best fit are listed in Table 5. Note that only one ω and one n value give a good match to the experimental data due to unique nature of this function. The uniqueness of this function was illustrated in Babadagli et al. (2005). The same study also showed that there is a strong correlation between the time value, at which 50% of recoverable oil was recovered, and ω. Therefore, we first tested the existence of this correlation. Figure 13 shows the plot of $t_{50\%}$ versus ω for all fluid pairs under both ultrasound and without ultrasound. The constant value of 0.69 in the function of y-axis is due to natural log value of 0.5, which corresponds to the recovery value at which the time value was taken. As shown, all points line up on a straight-line relationship yielding a correlation with the coefficients close to one. This indicates that the exponential function in Eq. 1 models the capillary imbibition behavior and the error generated by applying this model is minimal.

With the justification obtained from the plot in Fig. 13, we can further analyze the parameters in this function. We observe that n is much less affected by ultrasound than ω (Figs. 14, 15). A good agreement is observed between the n values of runs with ultrasound versus no ultrasound. This is an expected outcome as n is the "tuning parameter", which is mainly related to the recovery rate (Babadagli et al. 2005), and the recovery rate (mainly controlled by the wettability and permeability) was not significantly affected by the ultrasonic energy as can be seen through the curves in Fig. 16. The function $f(\gamma,\theta)$ shown in Fig. 16 was obtained from the slope of a straight line fit of Q^2 versus time. Handy (1960) suggested that the time dependence of the imbibition rate into uncoated rocks follows

$$Q^2 = \left(\frac{2P_{c,\mathrm{eff}} k_w \phi A^2 S_w}{\mu_w}\right) t \propto f(\gamma,\theta) * t \tag{2}$$

Table 5 Data used in the multi-variable regression analysis

	$f(\gamma,\theta)$	$t_{50\%}$ (mins)	$(\omega/0.69)^{1/n}$	n	Recovery (%PV)
With ultrasound					
B1	–	20	0.054	0.54	54%
L1	–	11	0.091	0.72	37%
7A	0.292	6	0.161	0.93	50%
8A	0.317	8	0.124	0.81	58%
3A	0.192	13	0.076	0.93	49%
4A	0.091	17	0.059	1.24	37%
5A	0.057	35	0.028	0.66	55%
9A	0.191	8.42	0.123	1.28	45%
10A	0.072	22	0.057	0.67	54%
1_2	0.201	200	0.006	2.76	35%
2¯2	0.260	185	0.005	3.88	39%
M̄2	0.157	40	0.038	1.24	57%
MM2	0.067	45	0.025	1.05	53%
P2	0.080	45	0.024	0.79	58%
G2	0.169	30	0.031	1.16	56%
LL2	0.049	110	0.009	0.53	63%
F2	0.027	135	0.008	0.55	55%
H2	0.039	95	0.011	0.58	61%
D2	0.054	80	0.013	0.61	58%
E2	0.063	50	0.021	0.49	62%
B3	0.0023	2800	0.0004	1.94	23%
B1b	0.15	160	0.006	1.53	48%
Without ultrasound					
B2	–	17	0.058	0.44	47%
L2	–	28	0.036	0.78	63%
7B	0.354	8	0.128	0.77	63%
8B	0.293	10	0.104	0.85	57%
3B	0.061	20	0.049	0.93	35%
4B	0.104	15	0.068	1.25	36%
5B	0.048	35	0.030	0.61	44%
9B	0.079	21	0.045	1.00	43%
10B	0.064	24	0.051	0.98	51%
1_1	0.214	195	0.005	3.06	32%
2¯1	0.237	200	0.005	3.57	35%
M̄1	0.100	45	0.028	1.14	47%
MM1	0.053	48	0.024	1.03	49%
P1	0.100	45	0.028	1.14	47%
G1	0.175	38	0.027	1.33	56%
K2	0.025	140	0.008	0.57	61%
F1	0.032	130	0.008	0.57	65%
H1	0.029	135	0.008	0.61	59%
D1	0.065	40	0.026	0.76	48%
E1	0.065	110	0.009	0.83	51%
B4	0.0052	2100	0.0005	0.92	50%
B2b	0.1041	230	0.004	1.74	49%

The exponential coefficients ω and η were obtained by fitting the function (Eq. 1) to the experiments (Fig. 2). The capillary function $f(\gamma,\theta)$ and the time required to recover the 50% of recoverable oil $t_{50\%}$ and ultimate recoveries were also added

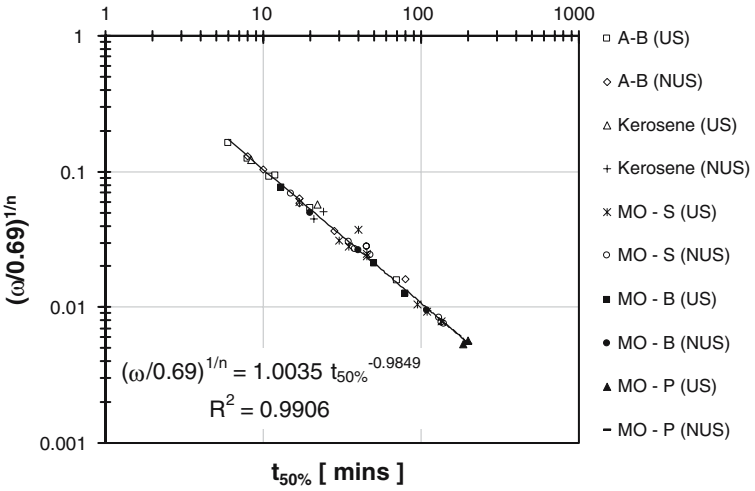

Fig. 13 Diagnostic plot illustrating that the exponential model in Eq. 1 is useful in describing the experimental data. The abbreviations US and NUS represent experimental data with ultrasound and without ultrasound, respectively. Other abbreviations are as defined in Table 3

where $P_{c,\text{eff}}$ denotes the effective capillary pressure that is a measure of the wettability of the rock sample. The function, $f(\gamma,\theta)$, used in our analysis corresponds to slope between Q^2 and t in Eq. 2 and may be used by Babadagli to quantify the capillary pressure (1996). All other parameters such as k_w, A, μ_w and the pore size distribution are assumed to be the same for cores under ultrasound and without ultrasound. Therefore, it is possible to use the slope of the straight-line segment of the Q^2 versus time plot to represent $\gamma\cos(\theta)$. It is difficult however whether the observed changes are due to γ or wettability. Figure 16 shows a plot of observed capillary function, $f(\gamma,\theta)$ without ultrasound versus with ultrasound. We observe that $f(\gamma,\theta)$ was not considerably affected by the presence of ultrasound for most of the fluid pairs. The only fluid pairs that showed a deviation were mineral oil–surfactant (1%) of 500 md Berea sandstone (M1, M2), kerosene–water (9A, 9B), and mineral oil–brine of 200 md Berea sandstone (3A, 3B). Having only three pairs showing lower water wettability out of 24 experiments gives us confidence to conclude that no significant change in the wettability is expected when ultrasonic energy is applied. The deviations for the three cases can be considered within the acceptable error margin of the experimental measurements. This also could be caused by some variability in the properties of the rock samples used.

For the other parameter ω, significant deviations are observed. It is believed that ω is a function of other rock and fluid properties including IFT, wettability, and core dimensions etc (Babadagli et al. 2005). It can be seen in Fig. 15 that all high IFT fluid pairs deviate from "unchanged", experiencing an increase in ω. An alteration of viscosity is most likely not the origin of the strong variation in ω, since great care was taken to maintain a constant temperature in the ultrasonic bath. In the case of mineral oil–brine the viscosity ratio is approximately 37, while for kerosene–brine, the viscosity ratio is close to two. The air–water pairs have a viscosity ratio of 0.02. It is observed that the effect of ultrasound on ω is very similar regardless the viscosity ratio. One key similarity between the fluid pairs showing strong deviation of

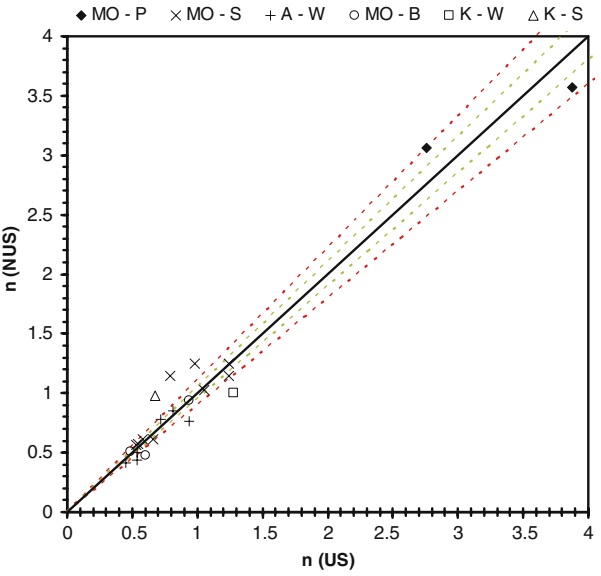

Fig. 14 Plot of exponential parameter n at undisturbed condition (NUS) versus imbibition by ultrasound for various fluid pairs. Dashed lines indicate ±10% and ±20% deviation from "no difference", represented as the solid line

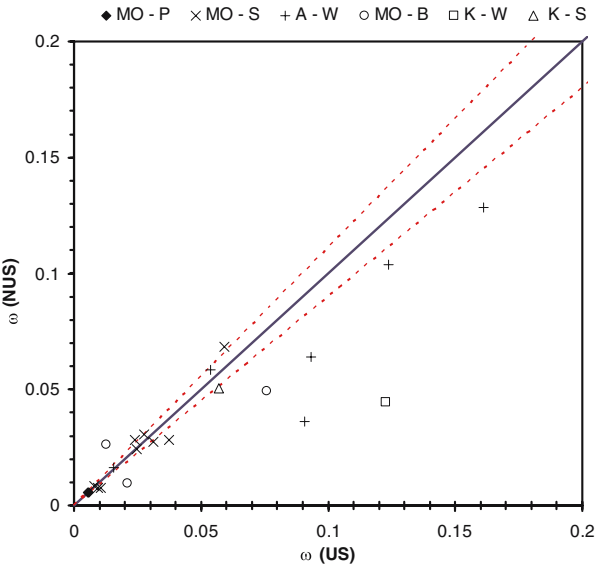

Fig. 15 Plot of exponential parameter ω at undisturbed condition (NUS) versus imbibition by ultrasound (US) for various fluid pairs. Dashed lines indicate ±10% deviation from "no difference", represented as the solid line

ω (mineral oil–brine, kerosene–brine and air–water) is high interfacial tension. Note that ω for kerosene–brine (high IFT) strongly deviates from "unchanged", while ω for kerosene-surfactant (low IFT) is unchanged. A similar behavior was observed with the mineral oil case. This indicates that interfacial tension may be the most dominant factor on increasing ω under ultrasonic radiation. For low IFT fluid pairs, ultrasound does not seem to have a measurable effect on the transport mechanism within porous media. However, for high IFT fluid pairs, it was observed that ultrasound reduced IFT and therefore capillary pressure.

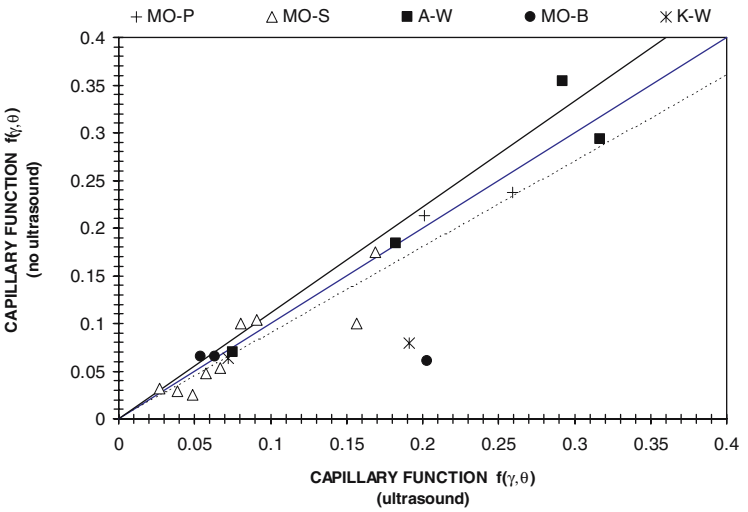

Fig. 16 Plot of capillary function of undisturbed (NUS) imbibition versus imbibition by ultrasound (US) for various fluid pairs. Dashed lines indicate ±10% deviation from "no difference", represented as the solid line

5 Conclusions

1. Capillary imbibition recovery performances of the Berea sandstone samples saturated with mineral oil and kerosene for brine, surfactant and polymer solutions were studied under ultrasound. Ultrasound may either improve or deteriorate production of oil by imbibition, depending on the selection of aqueous phase, oleic phase and ultrasonic intensity. In general, all cases except counter-current kerosene–water imbibition in Berea sandstone and co-current air–water in Indiana limestone ultrasound showed significant improvements in oil recovery.
2. To explain the observed enhancements in recovery of oil–surfactant fluid pairs, we postulate that ultrasound may enhance surfactant solubility and reduce adsorption in Berea sandstone. This conjecture must however be tested with more elaborate tests.
3. Recovery of oil under ultrasound using viscosity enhancing agents such as Xanthan gum depends on polymer concentration. At higher polymer concentrations, lower recovery with increasing intensity was obtained. This implies that there is an optimal value of ultrasonic intensity.
4. Ultrasound does not seem to have a major effect on capillary pressure. We observe an implicit relationship between interfacial tension and the exponential parameter ω of Eq. 1 which governs capillary imbibition recovery. High IFT fluid pairs did show a clear deviation from the "no ultrasound" case. The major contribution from ultrasonic energy on the incremental recovery is due to change in the interfacial action between the aqueous and non-wetting phase. Further investigation is required to determine whether this change is due to an alteration of IFT under ultrasonic effect or causes related to rock-fluid interaction due to vibration.

Acknowledgements This study was partly funded by an NSERC Grant (No: G121210595). The funds for the equipment used in the experiments were obtained from the Canadian Foundation for Innovation (CFI) (Project # 7566) and the University of Alberta. We gratefully acknowledge these supports. We also would like to thank Sean Watt for his assistance and Can Ulas Hatiboglu for his advice during the experimental work. This paper is the revised and improved version of SPE 92124 and SPE 94105 presented at the Asia Pacific Oil & Gas Conference and Exhibition held in Jakarta, Indonesia, 5–7 April 2005 and SPE EUROPEC Conference, held in Madrid, Spain, 13–16 June 2005, respectively.

References

Aarts, A.C.T.,, Ooms, G.: Net flow of compressible viscous liquids induced by traveling waves in porous media. J. Eng. Math. **34**, 435–450 (1998)

Aarts, A.C.T. et al.: Enhancement of liquid flow through a porous medium by ultrasonic radiation. SPE J. **5**, 321 (1999)

Abismail, B. et al.: Emulsification by ultrasound: drop size distribution and stability. Ultrasonics Sonochem. **6**, 75–83 (1999)

Babadagli, T.: Temperature effect on heavy–oil recovery by imbibition in fractured reservoirs. J. Pet. Sci. Eng. **14**, 197 (1996)

Babadagli, T., Hatiboglu, C.U., Hamida, T.: Evaluation of matrix-fracture transfer functions for counter-current capillary imbibition. SPE 92111, SPE Asia Pacific Oil & Gas Conf. and Exh., 12–14 April 2005, Jakarta, Indonesia (2005)

Beresnev, I.A., Johnson, P.A.: Elastic-wave stimulation of oil production: a review of methods and results. Geophysics **59**(6), 1000–1017 (1994)

Biot, M.A.: Theory of propagation of elastic waves in a fluid-saturated porous solid: I. Low-frequency range. J. Acoust. Soc. Am. **28**, 168–178 (1956a)

Biot, M.A.: Theory of propagation of elastic waves in a fluid-saturated porous solid: II. Higher-frequency range. J. Acoust. Soc. Am. **28**, 179–191 (1956b)

Bjerknes, V.F.K.: Fields of force. Columbia University Press, New York (1906)

Buckingham, M.J.: Theory of compressional and transverse wave propagation in consolidated porous media. J. Acoust. Soc. Am **106**, 575–581 (1999)

Champion, B., van der Bas, F., Nitters, G.: The application of high-power sound waves for wellbore cleaning. SPE Product. Facilit. **19**(3), 113–121 (2004)

Cherskiy, N.V., Tsarev, V.P., Konovalov, V.M., Kusnetsov, O.L.: The effect of ultrasound on permeability of rocks to water. Trans. (Doklady) of the USSR Acad. Sci., Earth Sci. Sect. **232** 201–204 (1977)

Cil, M. et al.: An examination of countercurrent capillary imbibition recovery from single matrix blocks and recovery predictions by analytical matrix/fracture transfer functions. SPE 49005, 1998 SPE Annual Tech. Conf. and Exh., New Orleans, LA, 27–30 Sept. (1998)

Dezhkunov, N.V., Leighton, T.G.: Study into correlation between the ultrasonic capillary effect and sonoluminescence. J. Eng. Phys. Thermophys. **77**(1), 53–61 (2004)

Duhon, R.D., Campbell, J.M.: The effect of ultrasonic energy on the flow of fluids in porous media. SPE 1316, presented at the 2nd Annual Eastern Regional Meeting of SPE/AIME, Charleston, WV, Nov. 4–5 (1965)

Dyblenko, V.P. et al.: Percolation phenomena and processes in saturated porous media under the vibro-wave action, in ways of intensification of oil production (Putu intensifikatsii dobychi nefti). Proc. (Trudy) Basharki Res. Design Inst. Oil (Bashnipineft) 45–51 (1989) (in Russian)

Ellingsen, O. et al.: Process to increase petroleum recovery from petroleum reservoirs. U.S. patent 5,282,508

Fairbanks, H.V., Chen, W.I.: Ultrasonic acceleration of liquid flow through porous media. Chem. Eng. Prog. Symp. Ser. **67**, 108–116 (1971)

Gadiev, S.M.: Use of Vibrations in Oil Production (Ispol'zovaniye vibratsii v dobyche nefti). Nedra Press (1977) (in Russian)

Graham, D.R., Higdon, J.J.L.: Oscillatory flow of droplets in capillary tubes. Part 1. Straight tubes. J. Fluid Mech. **425**, 31–53 (2000a)

Graham, D.R., Higdon, J.J.L.: Oscillatory flow of droplets in capillary tubes. Part 2. Constricted tubes. J. Fluid Mech. **425**, 55–77 (2000b)

Graham, D.R., Higdon, J.J.L.: Oscillatory forcing of flow through porous media. Part 1. Steady flow. J. Fluid Mech. **465**, 213–235 (2002a)
Graham, D.R., Higdon, J.J.L.: Oscillatory forcing of flow through porous media. Part 2. Unsteady flow. J. Fluid Mech. **465**, 237–260 (2002b)
Guo, X. et al.: High frequency vibration recovery enhancement technology in the heavy oil fields of China. SPE 86956, Presented at the SPE Int. Thermal Operations and Heavy Oil Symposium and Western Regional Meeting, Bakersfield, CA, Mar. 16 –18 (2004)
Hamida, T., Babadagli, T.: Effects of ultrasonic waves on immiscible and miscible displacement in porous media. SPE 95327, 2005 SPE Annual Technical Conference and Exh., Dallas, TX, 9–12 Oct. (2005)
Hamida, T., Babadagli, T.: Investigations on capillary and viscous displacement under ultrasonic waves. J. Can. Petrol. Technol. **45**(2), 16–19 (2006)
Handy, L.L.: Determination of effective capillary pressure for porous media from imbibition data. Trans. AIME **219**, 75 (1960)
Herskowitz, M., Levitsky, S., Shreiber, I.: Attenuation of ultrasound in Porous media with dispersed microbubbles. Ultrasonics **38**, 767 (2000)
Hilpert, M., Jirka, G.H., Plate, E.J.: Capillarity-induced resonance of oil bLOBS iN capillary tubes and porous media. Geophysics **65**(3), 874 (2000)
Iovenitty, J.L. et al.: Acoustically enhanced remediation: phase II–technology scaling. Presented at 1996 DOE Conference on Industry Partnerships to Deploy Environmental Technology, Oct. 22–24 (1996)
Kim, Y.U., Wang, M.C.: Effect of ultrasound on oil removal from soils. Ultrasonics **41**, 539–542 (2003)
Krylov, A.L., Nikolaevskiy, V.N., El', G.A.: Mathematical model of nonlinear generation of ultrasound by seismic waves. Trans. USSR Acad. Sci. **318**(6), 1339–1345 (1991)
Lawson, J.B.: The adsorption of non-ionic surfactants on sandstone and carbonate. SPE 7052, 1978 SPE Symposium on Improved Methods for Oil Recovery, Tulsa, OK
Li, W. et al.: Vibration-induced mobilization of trapped oil ganglia in porous media: experimental validation of a capillary-physics mechanism. J. Colloid Interface Sci. **289**, 193–199 (2005)
Mannhardt, J.J.N., Jha, K.N.: Adsorption of foam-forming surfactants in Berea sandstone. JCPT **33**(2), 34 (1994)
Metting, R. et al.: Bjerknes forces between small cavitation bubbles in a strong acoustic field. Phys. Rev. E **56**, 2924–2931 (1997)
Meyer, R.J. et al.: Method for improving oil recovery using and ultrasound technique. U.S. patent 6,405,796 B1
Mikhailov, V.M. et al.: Study of ultrasonic effect on percolation process in porous media. Proc. (Trudy) All Union Res. Inst. Nuclear Geophys. Geochem. **24**, 78–87 (1975)
Moholkar, V.S., Warmoeskerken, M.M.C.G.: Investigations in mass transfer enhancement in textiles with ultrasound. Chem. Eng. Sci **59**, 299–311 (2004)
Neretin, V.D., Yudin, V.A.: Results of experimental study of the influence of acoustic treatment on percolation processes in saturated porous media. In: Topics in Nonlinear Geophysics (Voprosi nelineinoy geofisiki): All Union Research Institute of Nuclear Geophysics and Geochemistry, pp. 132–137 (1981) (in Russian)
Nikolaevskiy, V.N.: Mechanism of vibroaction for oil recovery from reservoirs and dominant frequencies. Trans. USSR Acad. Sci. **307**, 570–575 (1989)
Pechkov, A.A. et al.: Acoustic flow stimulation method and apparatus. U.S. patent 5,184,678
Poesio, P. et al.: Removal of small particles from a porous material by ultrasonic irradiation. Transport Porous Media **54**, 239–264 (2004)
Roberts, P.M., Venkitaraman, A., Sharma, M.M.: Ultrasonic removal of organic deposits and polymer-induced formation damage. SPE Drill. Comp. **15**, 19 (2000)
Rozina, E.Y.: Effect of pulsed ultrasonic field on the filling of a capillary with a liquid. Colloid J. **64**(3), 359 (2003)
Rozina, E.Y., Rosin, Y.P.: About the nature of the sound capillary pressure. Presented at the XIII Session of the Russian Acoustical Society, Moscow, Aug. 25–29 (2003)
Trogus, F.J., Sophany, T., Schechter, R.S., Wade, W.H.: Static and dynamic adsorption of anionic and nonionic surfactants. SPEJ **17**(5), 337–344 (1977)
Varadaraj, R., Zushma, S., Brons, N.: Influence of surfactant structure on wettability modification of hydrophobic granular surfaces. J. Colloid Interface Sci. **167**, 207–210 (1994)
Venkitaraman, A., Roberts, P.M., Sharma, M.M.: Ultrasonic removal of near-wellbore damage caused by fines and Mud solids. SPE Drill. Comp. **10**(3), 193–197 (1995)

Wegener et al.: Methods and apparatus for enhancing well production using sonic energy. U.S. patent 6,186,228 B1
Wegener et al.: Heavy oil viscosity reduction and production. U.S. patent 6,279,653 B1
Wong, S.W. et al.: Near wellbore stimulation by acoustic waves. SPE 82198, 2003 SPE European Formation Damage Conference, The Hague, Netherlands, 13–14 May (2003)
Wong, S.W. et al.: High-power/high-frequency acoustic stimulation: a novel and effective wellbore stimulation technology. SPE Product. Facilit. 183 (2004)